Chapter 2
Mechanical Theory of the Film-on-Substrate-Foil Structure: Curvature and Overlay Alignment in Amorphous Silicon Thin-Film Devices Fabricated on Free-Standing Foil Substrates

Helena Gleskova, I-Chun Cheng, Sigurd Wagner, and Zhigang Suo

Abstract   Flexible electronics will have inorganic devices grown at elevated temperatures on free-standing foil substrates. The thermal contraction mismatch between the substrate and the deposited device films, and the built-in stresses in these films, cause curving and a change in the in-plane dimensions of the workpiece. This change causes misalignment between the device layers. The thinner and more compliant the substrate, the larger the curvature and the misalignment. We model this situation with the theory of a bimetallic strip, which suggests that the misalignment can be minimized by tailoring the built-in stress introduced during film growth. Amorphous silicon thin-film transistors (a-Si:H TFTs) fabricated on stainless steel or polyimide (PI) (Kapton E®) foils need tensile built-in stress to compensate for the differential thermal contraction between the silicon films and the substrate. Experiments show that by varying the built-in stress in just one device layer, the gate silicon nitride (SiN_x), one can reduce the misalignment between the source/drain and the gate levels from ~400 parts-per-million to ~100 parts-per-million.

2.1 Introduction

Flexible displays built on metallic or plastic foil substrates are becoming a reality. Many flat panel display companies around the world have manufactured flexible display prototypes using a variety of thin-film technologies [1].

   The inorganic device films are typically grown at an elevated temperature while the substrate is held flat. Upon cooling, a stress field arises due to the difference

H. Gleskova (✉)
Department of Electronic and Electrical Engineering, University of Strathclyde, Royal College Building, Room 3.06A, 204 George Street, Glasgow, G1 1XW, UK
e-mail: helena.gleskova@eee.strath.ac.uk

in thermal contraction between the film and the substrate. If the substrate is thick and stiff, for example a silicon wafer or a plate of glass, the film-on-plate structure remains almost flat (it forms a spherical cap with a very large radius of curvature), even when the stress is large. The stress in the film is much bigger than in the substrate. If the stress in the film becomes too large or the bond between the film and the substrate is weak, the film may crack or peel off the substrate [2].

When the substrate's thickness is reduced, its strength, the product of thickness with Young's modulus, may become comparable to that of the deposited device film. Upon cooling, such a film-on-substrate-foil structure rolls to a cylinder with the film facing outward (film in compression) or inward (film in tension). When flattened for circuit fabrication, the workpiece has a different size from before film deposition. This change in size leads to an error in mask overlay alignment.

In flexible electronics, the rigid plate glass substrate of current liquid crystal displays is replaced with plastic or metallic foils. Among metallic materials, stainless steel, molybdenum, and aluminum foils have been utilized as substrates in the fabrication of thin-film transistors and solar cells. A number of plastic (organic polymers) substrates have also been tested successfully in a variety of thin-film applications. Table 2.1 lists the thermo-mechanical properties of the common foil substrates and of silicon nitride (SiN_x) and hydrogenated amorphous silicon (a-Si:H) deposited by plasma enhanced chemical vapor deposition (PECVD).

Foil substrates with thicknesses ranging from a few to several hundred micrometers were either free-standing during the whole fabrication process, or temporarily

Table 2.1 Thermo-mechanical properties of substrates used for flexible electronics, and of some TFT materials

Material	Brand name	Upper working temperature (°C)	Young's modulus (GPa)	CTE (K^{-1})	Source
Stainless steel	AISI 304	~1,400	190–210	18×10^{-6}	Goodfellow
Polyethylene naphthalate (PEN)	Kaladex, Kalidar	155	5–5.5	21×10^{-6} (biaxial)	Goodfellow
Polyethylene terephthalate (PET)	Arnite, Dacron, Mylar, etc.	115–170	2–4	$30–65 \times 10^{-6}$	Goodfellow
Polyimide (PI)	Kinel, Upilex, Upimol, etc.	250–320	2–3	$30–60 \times 10^{-6}$	Goodfellow
Polyimide (PI)	Kapton E®	>300	5.2	16×10^{-6}	DuPont
PECVD silicon nitride	–	–	183	2.7×10^{-6}	[3, 4]
PECVD amorphous silicon	–	–	140	3.0×10^{-6}	[5]

attached to a carrier during the fabrication and separated after the fabrication was completed. Each approach faces different challenges. We focus on the mechanics of thin-film devices fabricated on free-standing foils because of our experience with them, and because of their relevance to roll-to-roll processing. The simple thermo-mechanical theory introduced in this chapter addresses two important issues that arise when the device films are deposited on the foil substrates at an elevated temperature: (1) the change in the dimensions of the flattened workpiece and (2) the curving of the workpiece.

Mechanical strain is defined as a relative change in dimensions. Therefore, the terms *change in dimensions* and *strain* are interchangeable and they both require a reference point. For any given temperature, the substrate and the film have different reference points: they are their respective in-plane dimensions, were they relaxed instead of bonded together. For example in Fig. 2.1 , $\varepsilon_s(T_d) < 0$, $\varepsilon_f(T_d) > 0$,
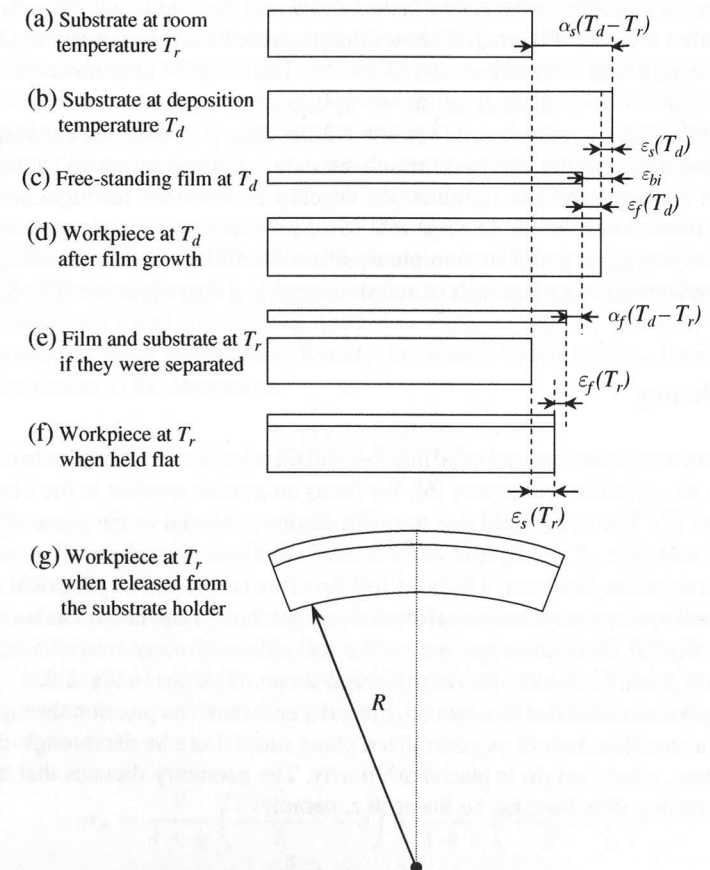

Fig. 2.1 Length or width of a film-on-foil structure at room and growth temperatures

$\varepsilon_s(T_r) > 0$, and $\varepsilon_f(T_r) < 0$, where the subscripts s and f are for the substrate and film, respectively, and T_d and T_r are for deposition and room temperatures, respectively.

Figure 2.1d represents a film grown on a free-standing foil substrate at an elevated temperature. The substrate is held flat during film growth. It expands when heated to the deposition temperature but remains stress-free (Fig. 2.1b). The growing film may develop a built-in strain ε_{bi} (Fig. 2.1c) that causes a built-in stress σ_{bi}. The built-in strain arises from atoms deposited in out-of-equilibrium positions. If the substrate is not constrained, the built-in strain ε_{bi} in the film forces the substrate to shrink or expand. Figure 2.1d depicts film with a built-in tensile stress ($\sigma_{bi} > 0$), which forces the substrate into compression ($\varepsilon_s(T_d) < 0$). Next, the unconstrained workpiece is cooled to room temperature. Since the coefficient of thermal expansion (CTE) of the device film, α_f, is typically much smaller than that of the substrate, α_s, the substrate wants to shrink more than the film, forcing the workpiece to roll into a cylinder with the film on the outside (Fig. 2.1g). When flattened for photolithographic alignment, the film and the substrate have the same in-plane dimensions. These dimensions are, however, different from those that the substrate and the film would have, were they not bonded together. Figure 2.1f shows that the substrate is in tension ($\varepsilon_s(T_r) > 0$), while the film is in compression ($\varepsilon_f(T_r) < 0$). The cause of alignment error, $\varepsilon_s(T_r)$, and the radius of curvature, R, of the workpiece are correlated.

For this chapter, we adapt in Section 2.2 the theory of a bimetallic strip to calculate the strains in the film and the substrate during film growth and after cooling to room temperature. The formulae we develop can be used for any combination of film/substrate materials. In Section 2.3, we provide a specific, quantitative guide to controlling $\varepsilon_s(T_r)$ and R in amorphous silicon thin-film transistors (a-Si:H TFTs) fabricated on free-standing foils of stainless steel and the polyimide (PI), Kapton E.

2.2 Theory

Several recent papers have adapted the classical theory of bimetallic strips to integrated circuits on crystalline substrates [6]. We focus on aspects specific to the film-on-foil structure [7]. The stress field due to misfit strains is biaxial in the plane of the film and the substrate. A small, stiff wafer bends into a spherical cap with an equal and biaxial curvature. However, a film-on-foil structure bends into a cylindrical roll. The transition from cap to roll as the substrate becomes thinner and larger has been studied extensively [6]. Foil substrates are on the roll side well away from the cap-to-roll transition point. They bend into a cylindrical shape, as shown in Fig. 2.2.

The strain in the axial direction, ε_A, is independent of the position throughout the sheet – a condition known as generalized plane strain. Let z be the through-thickness coordinate, whose origin is placed arbitrarily. The geometry dictates that the strain in the bending direction, ε_B, be linear in z, namely:

$$\varepsilon_B = \varepsilon_0 + \frac{z}{R} \tag{2.1}$$

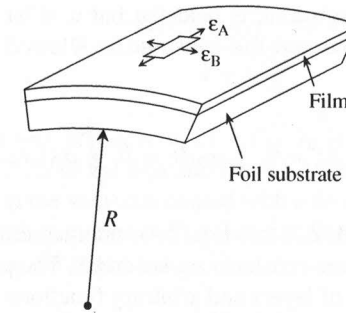where ε_0 is the strain at $z = 0$.

Fig. 2.2 A film-on-foil structure bends into a cylindrical roll [7]. This illustration corresponds to Fig. 2.1(g)

If the film and the substrate were separated, they would strain by different amounts but develop no stress (Fig. 2.1e). Let e be the strain developed in an unconstrained stress-free material. For example, thermal expansion produces a strain $e = \alpha \Delta T$, where α is the CTE, and ΔT, the temperature change (Fig. 2.1b). One may also include in e the built-in strain ε_{bi} (Fig. 2.1c). Now, if the film and the substrate are bonded to each other and cannot slide relative to each other, a stress field arises (Fig. 2.1d, f). The two stress components in the axial and the bending directions, σ_A and σ_B, are both functions of z (Figs. 2.1g and 2.2). Each layer of the material is taken to be an isotropic elastic solid with Young's modulus Y and Poisson ratio ν, and obeys Hooke's law $\sigma = Y\varepsilon$. (Uniaxial tensile stress along the x-axis of a free-standing sample causes stretch along the x-direction coupled with shrinkage along the unconstrained y and z directions, thus $\nu = -\varepsilon_y/\varepsilon_x = -\varepsilon_z/\varepsilon_x$.) The film and the substrate are dissimilar materials: e, Y, and ν are known functions of z. Hooke's law relates the strains to the stresses as:

$$\varepsilon_A = \frac{\sigma_A}{Y} - \nu\frac{\sigma_B}{Y} + e \tag{2.2a}$$

$$\varepsilon_B = \frac{\sigma_B}{Y} - \nu\frac{\sigma_A}{Y} + e \tag{2.2b}$$

The first term on the right-hand side is the strain caused by stress applied in the same direction in which the strains ε_A and ε_B are measured, the second term is the strain due to stress applied in the perpendicular in-plane direction, and e is the strain developed in a stress-free material. Any changes in z-direction are neglected. Equation (2.2) can be modified to:

$$\sigma_A = \frac{Y}{1-\nu}\left(\frac{\varepsilon_A + \varepsilon_B}{2} - e\right) + \frac{Y}{1+\nu}\left(\frac{\varepsilon_A - \varepsilon_B}{2}\right) \tag{2.3a}$$

$$\sigma_B = \frac{Y}{1-\nu}\left(\frac{\varepsilon_A + \varepsilon_B}{2} - e\right) - \frac{Y}{1+\nu}\left(\frac{\varepsilon_A - \varepsilon_B}{2}\right) \tag{2.3b}$$

During film growth, the substrate is held flat but it is let loose upon cooling. No external forces are applied and the substrate is allowed to bend. Force balance requires that:

$$\int \sigma_A dz = 0, \quad \int \sigma_B dz = 0, \quad \int \sigma_B z \, dz = 0. \tag{2.4}$$

By inserting Eqs. (2.1) and (2.3) into Eq. (2.4) and integrating, we obtain three linear algebraic equations for three constants ε_A, ε_0, and R. The procedure outlined here is applicable to any number of layers and arbitrary functions $e(z)$, $Y(z)$, and $v(z)$.

When the film and the substrate are bonded together and are forced to be flat, the strains in the substrate and the film are equal at all times, and $\varepsilon_A = \varepsilon_B = \varepsilon$ (see Fig. 2.3). The corresponding stress components are also equal, $\sigma_A = \sigma_B$, but the stress in the substrate, σ_s, is different from that in the film, σ_f. In this case, Eq. (2.2) lead to:

$$\varepsilon = \frac{(1 - v_s) \cdot \sigma_s}{Y_s} + e_s = \frac{\sigma_s}{Y_s^*} + e_s \tag{2.5a}$$

$$\varepsilon = \frac{(1 - v_f) \cdot \sigma_f}{Y_f} + e_f = \frac{\sigma_f}{Y_f^*} + e_f \tag{2.5b}$$

where ε, σ, v, and Y are the strain, stress, Poisson ratio, and Young's modulus, respectively. $Y_f^* = \frac{Y_f}{1 - v_f}$ and $Y_s^* = \frac{Y_s}{1 - v_s}$ are the biaxial strain moduli of the film and the substrate, respectively.

For a flattened workpiece with no external in-plain force applied, Equations (2.4) lead to:

$$\sigma_f d_f + \sigma_s d_s = 0 \tag{2.6}$$

Equations (2.5) and (2.6) lead to an expression for the strain ε of the workpiece at an arbitrary temperature T:

$$\varepsilon_A = \varepsilon_B = \varepsilon$$
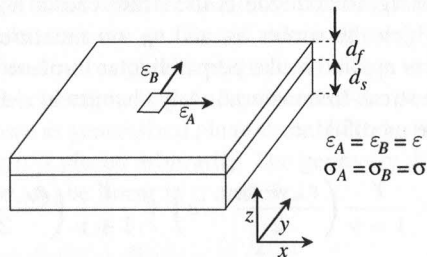$$\sigma_A = \sigma_B = \sigma$$

Fig. 2.3 Flattened film-on foil structure. This illustration corresponds to Fig. 2.1(**d**) and (**f**)

$$\varepsilon(T) = \frac{e_s(T) + \frac{Y_f^* d_f}{Y_s^* d_s} \cdot e_f(T)}{1 + \frac{Y_f^* d_f}{Y_s^* d_s}} \tag{2.7}$$

where $e_f = \alpha_f (T - T_d) + \varepsilon_{bi}$ and $e_s = \alpha_s (T - T_d)$. T_d is the deposition temperature, and α_f and α_s are the CTEs of the film and the substrate, respectively.

The in-plane strain in the substrate coated with a film (strain in the substrate of a flattened workpiece) with respect to the uncoated substrate at the same temperature, at any temperature T, can be expressed as:

$$\varepsilon_s(T) = \varepsilon(T) - e_s(T) = \frac{\left[(T_d - T)(\alpha_s - \alpha_f) + \varepsilon_{bi} \right]}{1 + \frac{Y_s^* d_s}{Y_f^* d_f}} \tag{2.8a}$$

Similarly, the in-plane strain in the film (strain in the film of a flattened workpiece) with respect to the free-standing film at the same temperature, at any temperature T, can be expressed as:

$$\varepsilon_f(T) = \varepsilon(T) - e_f(T) = -\frac{\left[(T_d - T)(\alpha_s - \alpha_f) + \varepsilon_{bi} \right]}{1 + \frac{Y_f^* d_f}{Y_s^* d_s}} \tag{2.8b}$$

2.2.1 The Built-in Strain ε_{bi}

The built-in strain ε_{bi} that develops in the film during its deposition manifests itself by the built-in stress σ_{bi}. At $T = T_d$, the only stress in the film is the built-in stress σ_{bi} and Eqs. (2.5) and (2.6) lead to:

$$\varepsilon_{bi} = -\frac{\sigma_{bi}}{Y_f^*} \cdot \left(1 + \frac{Y_f^* d_f}{Y_s^* d_s} \right) \tag{2.9}$$

The minus sign indicates that, at the deposition temperature, a film with built-in tensile stress ($\sigma_{bi} > 0$) forces the substrate to shrink, while a film with built-in compressive stress ($\sigma_{bi} < 0$) forces the substrate to expand. (If the deposition is done at room temperature, the film with built-in tensile stress forces the substrate into compression. If released, it will curve such that the film lies on the concave side.) The term in the parentheses is the modification for a compliant substrate: when the film strength, $Y_f^* d_f$, becomes comparable to the substrate strength, $Y_s^* d_s$, the substrate changes its dimension in response to film deposition. For stiff substrates when $Y_f^* d_f << Y_s^* d_s$, this term equals 1.

Both ε_{bi} and σ_{bi} can be complicated functions of the film's through-thickness coordinate z. Typically, neither $\varepsilon_{bi}(z)$ nor $\sigma_{bi}(z)$ is known. Therefore, an average strain value $\overline{\varepsilon_{bi}}$ is extracted from experiments for a given film/substrate couple, for example from the radius of curvature of the relaxed workpiece [8].

For the remainder of this chapter, we will use the built-in strain ε_{bi}. Remember that, following Eq. (2.9), the built-in strain is *negative if tensile built-in stress* is grown into the film, and it is *positive for compressive built-in stress*.

2.3 Applications

2.3.1 Strain in the Substrate, $\varepsilon_s(T_d)$, and the Film, $\varepsilon_f(T_d)$, at the Deposition Temperature T_d

A growing film typically builds in strain ε_{bi}. This built-in strain arises from atoms deposited in out-of-equilibrium positions. If the substrate is thin and/or compliant and unconstrained, the growing film will relieve some of its built-in strain/stress by forcing the substrate to shrink (tensile built-in stress in the film) or expand (compressive built-in stress in the film). The change in the substrate's in-plane dimensions (strain in the substrate of a flattened workpiece) at the deposition temperature T_d can be calculated from Eq. (2.8a) by setting $T = T_d$:

$$\varepsilon_s(T_d) = \frac{\varepsilon_{bi}}{1 + \frac{Y_s^* d_s}{Y_f^* d_f}} \tag{2.10}$$

Equation (2.10) compares the in-plane substrate's dimensions at the deposition temperature T_d after and before film growth. Tensile built-in strain ($\varepsilon_{bi} < 0$) leads to a negative $\varepsilon_s(T_d)$, indicating substrate shrinkage during film growth (see Fig. 2.1d). Compressive built-in strain ($\varepsilon_{bi} > 0$) leads to a positive $\varepsilon_s(T_d)$, indicating substrate expansion during film growth.

Setting $T = T_d$ in Eq. (2.8b) expresses the change in the in-plane film's dimensions (strain in the film of a flattened workpiece) at the deposition temperature T_d:

$$\varepsilon_f(T_d) = -\frac{\varepsilon_{bi}}{1 + \frac{Y_f^* d_f}{Y_s^* d_s}} \tag{2.11}$$

Equation (2.11) describes the in-plane strain in the film at the deposition temperature T_d when the built-in strain ε_{bi} is present (compared to the absence of ε_{bi}). Tensile built-in strain ($\varepsilon_{bi} < 0$) leads to a positive $\varepsilon_f(T_d)$, indicating that the film is stretched (see Fig. 2.1d). Compressive built-in strain ($\varepsilon_{bi} > 0$) leads to a negative $\varepsilon_f(T_d)$, indicating compression in the growing film.

$\varepsilon_s(T_d)$ and $\varepsilon_f(T_d)$ both equal zero if the film has no built-in strain/stress. For $\varepsilon_{bi} \neq 0$ and a thick and rigid substrate ($Y_f^* d_f \ll Y_s^* d_s$), all strain/stress is taken up by the film, $\varepsilon_f(T_d) = -\varepsilon_{bi}$, leaving the substrate free of strain and stress, $\varepsilon_s(T_d) \to 0$. For compliant substrates, the denominator in Eqs. (2.10) and (2.11) becomes a finite number larger than 1, indicating that the built-in strain is now divided between the film and the substrate depending on their relative strengths, $\frac{Y_f^* d_f}{Y_s^* d_s}$.
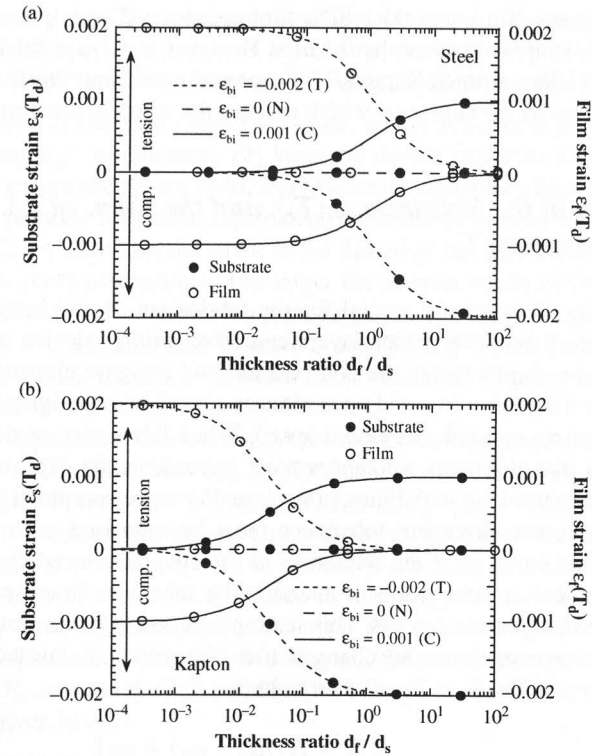
Fig. 2.4 Strain in the substrate, $\varepsilon_s(T_d)$, and the film, $\varepsilon_f(T_d)$, of a flattened workpiece at deposition temperature after deposition of SiN$_x$, as a function of film/substrate thickness ratio. (**a**) The upper frame is for steel ($Y_f^*/Y_s^* \cong 0.92$) substrate and (**b**) the lower frame for Kapton E ($Y_f^*/Y_s^* \cong 35$) substrate. The parameter ε_{bi} represents the built-in strains measured in SiN$_x$ films deposited by PECVD. T stands for built-tensile stress, C for built-in compressive stress, and N for no built-in stress in the film

Figure 2.4 shows examples of the calculated strain in the substrate and the film at the deposition temperature T_d as a function of the film/substrate thickness ratio. The upper frame is for steel, and the lower is for Kapton E. Three different values of the built-in strain ε_{bi}, -0.002 (T for tensile built-in stress), 0 (N for no built-in stress), and $+0.001$ (C for compressive built-in stress) were chosen to match the typical values of the built-in strain in SiN$_x$ films deposited by PECVD [8]. Other parameters used in the calculation are $Y_f^* = 183/(1-\nu)$ GPa, $Y_s^* = 200/(1-\nu)$ GPa (AISI 304 steel) or $5.2/(1-\nu)$ GPa (Kapton E), and $\nu = 0.3$ for both steel and Kapton E.

Strain develops in the film and the substrate at the deposition temperature only under built-in stress. When the film is very thin compared to the substrate, all strain/stress is taken up by the film and the substrate's dimensions do not change. With increasing film thickness, the strain in the film decreases and the strain in the

substrate increases. If a 1-μm-thick SiN_x film is deposited on a 100-μm-thick steel foil, almost all strain is taken up by the film. However, if a 1-μm-thick SiN_x film is deposited on a 100-μm-thick Kapton E foil, approximately one-fourth of the built-in strain is taken up by the substrate, which reduces the strain in the film.

2.3.2 Strain in the Substrate, $\varepsilon_s(T_r)$, and the Film, $\varepsilon_f(T_r)$, at Room Temperature T_r

Precise overlay alignment is crucial for the fabrication of any integrated circuit. Alignment errors between device layers can affect critical device tolerances, for example, the overlap between the source/drain and the gate electrodes in a TFT. Increasing the tolerances to avoid open circuits caused by misalignment raises parasitic capacitances and reduces circuit speed. When fabricating devices on a rigid plate of glass, the alignment tolerances must increase as the exposure frame size increases. When working with thinner (steel) and/or more compliant (organic polymer) substrates, the alignment tolerances must be increased even further. As a result, one must either raise the tolerances at the cost of reduced circuit speed, or use self-alignment, or find means to maintain the substrate dimensions unchanged throughout the fabrication process. This section analyzes how the dimensions of the substrate at room temperature are changed after film growth at elevated temperature.

By substituting $T = T_r$ in Eq. (2.8) we obtain:

$$\varepsilon_s(T_r) = \frac{\left[(T_d - T_r)(\alpha_s - \alpha_f) + \varepsilon_{bi}\right]}{1 + \frac{Y_s^* d_s}{Y_f^* d_f}} \tag{2.12}$$

$$\varepsilon_f(T_r) = -\frac{\left[(T_d - T_r)(\alpha_s - \alpha_f) + \varepsilon_{bi}\right]}{1 + \frac{Y_f^* d_f}{Y_s^* d_s}} \tag{2.13}$$

Equation (2.12) describes the strain of the substrate at room temperature, after film deposition at elevated temperature (Fig. 2.1f). It compares the in-plane dimensions of the flattened substrate/workpiece after and before film growth. For accurate overlay alignment, $\varepsilon_s(T_r)$ should be close to zero. $\varepsilon_s(T_r)$ can be made small by minimizing the numerator $\left[(T_d - T_r)(\alpha_s - \alpha_f) + \varepsilon_{bi}\right]$ and maximizing the denominator $1 + \frac{Y_s^* d_s}{Y_f^* d_f}$. This can be achieved by three ways:

(1) Choosing a substrate with a CTE close to that of the device layers. This is challenging for plastic substrates whose CTE usually is much larger than those of silicon device films.
(2) Minimizing $(T_d - T_r)$ by lowering the deposition temperature. In a-Si:H thin-film technology, lower deposition temperature leads to worse electronic properties. Here, organic electronics, for example polymer light-emitting diodes and thin-film transistors, have an advantage.

(3) Compensating the CTE mismatch with strain built into the device films, such that $\left[(T_d - T_r)(\alpha_s - \alpha_f) + \varepsilon_{bi} = 0\right]$. The built-in strain depends on the deposition conditions and sometimes can be easily adjusted (see Fig. 2.12).

One can also (1) choose a thicker substrate, which however is not desirable for flexing or "shaping" applications, (2) keep the device structure very thin, which however may reduce the device yield, and (3) choose substrate with a large Young's modulus (not possible for plastic substrates). These measures may be combined.

Equation (2.13) describes the strain in the film after the flattened workpiece has been cooled to room temperature. The larger the thermal misfit strain between the substrate and the film, $(T_d - T_r)(\alpha_s - \alpha_f)$, the larger the strain in the substrate and the film. When $\alpha_s > \alpha_f$, a tensile built-in strain in the film ($\varepsilon_{bi} < 0$) helps to compensate the thermal misfit and to reduce the strain in the substrate, which causes alignment error, and in the film, which causes film fracture.

Figure 2.5 depicts the strain of the substrate at room temperature, $\varepsilon_s(T_r)$, after film deposition, calculated from Eq. (2.12). Positive strain (tension) means that at room temperature the substrate is elongated after film growth, while negative strain (compression) indicates shrinkage. Three different values of the built-in strain in the film ε_{bi}, −0.002 (tensile built-in stress), 0 (no built-in stress), and +0.001 (compressive built-in stress), were chosen to match typical values of the built-in strain in SiN_x films deposited by PECVD [8]. The calculations are done for two different deposition temperatures $T_d = 150$ and $250°C$ for three types of substrates: steel, Kapton E, and a high-CTE plastic. The Young's modulus and CTE for each substrate are given below:

Young's modulus
Steel: $Y_s^* = 200/(1-\nu)$ GPa
Kapton E: $Y_s^* = 5.2/(1-\nu)$ GPa
High-CTE plastic: $Y_s^* = 3/(1-\nu)$ GPa
CTEs
Steel: $\alpha_s = 18 \times 10^{-6}$ K^{-1}
Kapton E: $\alpha_s = 16 \times 10^{-6}$ K^{-1}
High-CTE plastic: $\alpha_s = 40 \times 10^{-6}$ K^{-1}

In all cases, $Y_f^* = 183/(1-\nu)$ GPa, $\nu = 0.3$, $\alpha_f = 2.7 \times 10^{-6}$ K^{-1}, and $T_r = 20°C$. For the values of ε_{bi} used here, the steel substrate is seen to remain dimensionally stable ($\varepsilon_s(T_r) \cong 0$) up to $d_f/d_s \cong 0.01$, Kapton E up to $d_f/d_s \cong 0.0003$, and high-CTE plastic for $d_f/d_s < 0.0001$. It is clear that steel foil is dimensionally most stable during TFT processing. For all substrates, built-in tensile stress is preferable to compressive or no built-in stress because it can compensate differential thermal contraction. However, deposition on a high-CTE plastic foil causes a substantial elongation of the substrate regardless of the built-in stress in the film, even if the film is very thin ($d_f/d_s \sim 10^{-3}$). Note that brittle films withstand higher compressive strain than tensile strain, because tensile strain lower than $\sim 5 \times 10^{-3}$ may fracture the films. Yet fracture of device films is commonly observed on high-CTE plastics.

Figure 2.6 depicts the strain of the SiN_x film at room temperature, $\varepsilon_f(T_r)$, after its deposition at elevated temperature T_d, calculated from Eq. (2.13). Since all
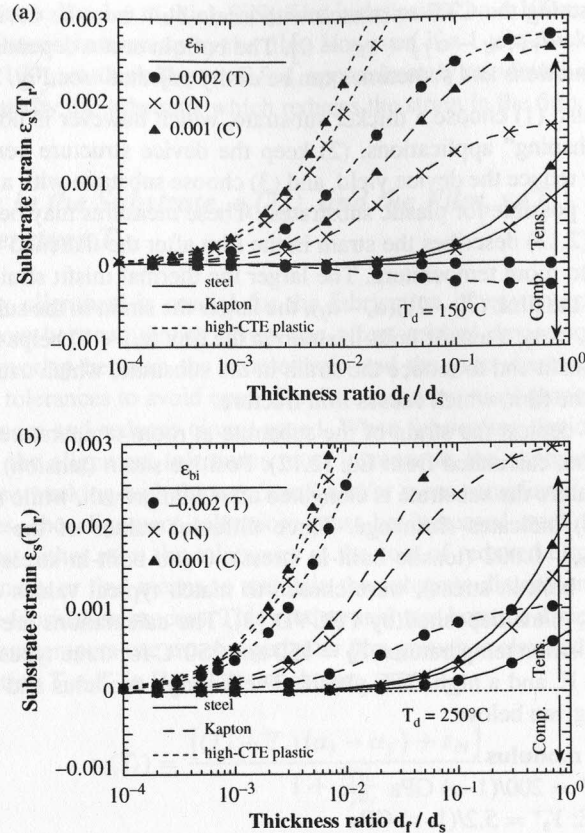
Fig. 2.5 Strain of the substrate at room temperature, $\varepsilon_s(T_r)$, after deposition of SiN_x, as a function of film/substrate thickness ratio. The three substrates illustrated are steel ($Y_f^*/Y_s^* \cong 0.92$, $\alpha_s = 18 \times 10^{-6}$ K^{-1}), Kapton E ($Y_f^*/Y_s^* \cong 35$, $\alpha_s = 16 \times 10^{-6}$ K^{-1}), and high-CTE plastic ($Y_f^*/Y_s^* \cong 45$, $\alpha_s = 40 \times 10^{-6}$ K^{-1}). The calculations are done for two different deposition temperatures: (a) $T_d = 150°$C and (b) $T_d = 250°$C. The parameter ε_{bi} is the built-in strain measured in SiN_x films deposited by PECVD. Other parameters are listed in the text. T stands for built-in tensile stress, C for built-in compressive stress, and N means no built-in stress in the film

substrates presented here have CTEs substantially larger than that of SiN_x film, when the flattened workpiece is cooled from the deposition temperature, the film is typically under compression. The compressive strain approaches 1% if the film is grown on a high-CTE plastic at 250°C. The strain in the film remains constant for steel up to $d_f/d_s \cong 0.03$, Kapton E up to $d_f/d_s \cong 0.001$, and high-CTE plastic for $d_f/d_s \cong 0.0001$, and it is partially relieved if thick films are grown.

The effect of the film's built-in strain ε_{bi} on substrate dimensions at room temperature, $\varepsilon_s(T_r)$, is shown in Fig. 2.7 for 100-μm-thick foil substrates after a 1-μm-thick SiN_x deposition at the temperatures of 150, 200, and 250°C. Positive strain (tension) means that at room temperature the substrate is elongated after film growth, negative strain (compression) indicates shrinkage. $\varepsilon_s(T_r)$, given by
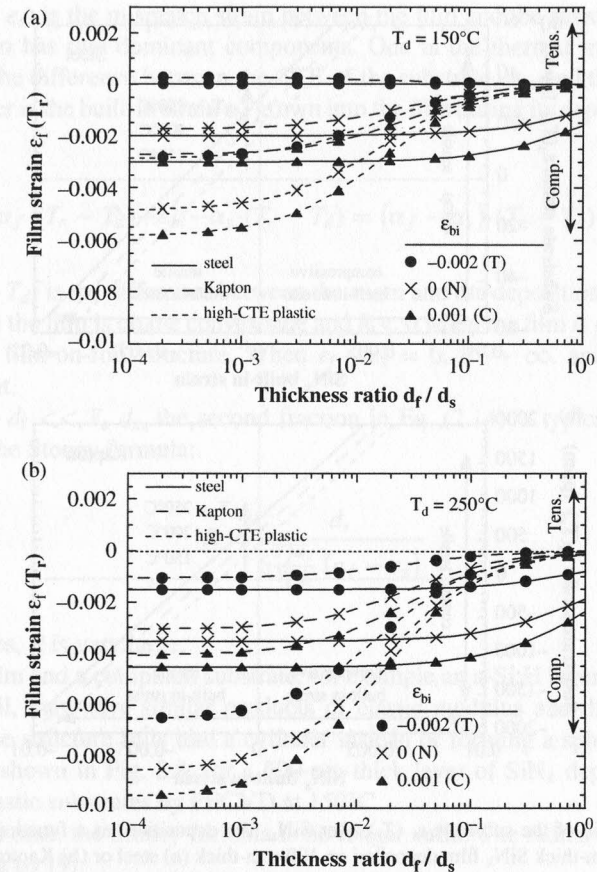

Fig. 2.6 Strain of the SiN_x film at room temperature, $\varepsilon_f(T_r)$, after its deposition at elevated temperature T_d, as a function of film/substrate thickness ratio. (a) $T_d = 150°$C and (b) $T_d = 250°$C. Parameters are the same as in Fig. 2.5

Eq. (2.12), is plotted as a function of the built-in strain in the film for steel (upper frame) and Kapton E (lower frame) substrates. As mentioned above, the film/substrate couple is held flat, as required for the alignment procedure. Because the CTE of steel and Kapton E are larger than that of SiN_x, both substrates are elongated after deposition and cooling if no built-in stress is grown into the film. The steel substrate is elongated by ~18 ppm for $T_d = 150°$C, by ~25 ppm for 200°C, and by ~32 ppm for 250°C; Kapton E by ~450 ppm for $T_d = 150°$C, by ~620 ppm for 200°C, and by ~800 ppm for 250°C. When the SiN_x film is grown with built-in *tensile* stress, $\varepsilon_s(T_r)$ is reduced. For $T_d = 250°$C for Kapton E, a built-in tensile strain of $\sim{-}3 \times 10^{-3}$ completely compensates the CTE mismatch between the substrate and the film, leaving the dimensions of the workpiece unchanged. Therefore, by tailoring the built-in strain/stress in the TFT layers, one can keep the film/substrate couple dimensionally stable for accurate photomask overlay alignment. Built-in
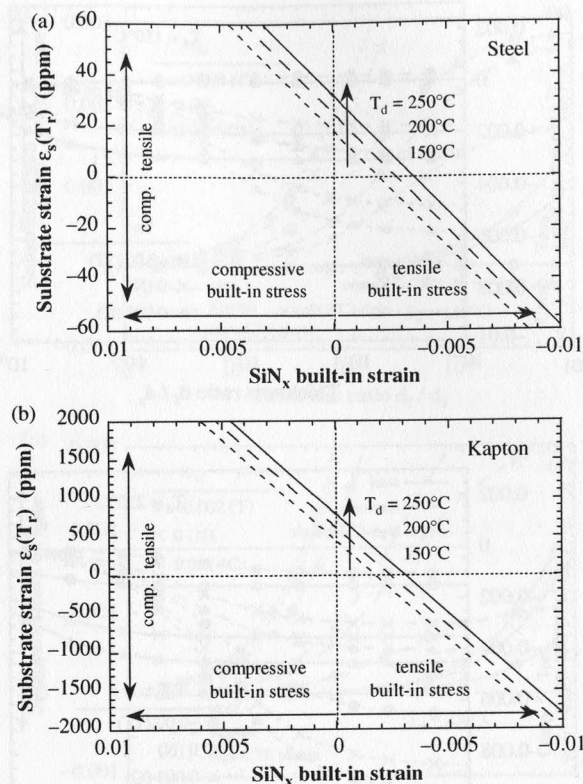
Fig. 2.7 Strain of the substrate ε_s (T_r) after SiN$_x$ film deposition, as a function of the built-in strain in a 1-μm-thick SiN$_x$ film deposited on 100-μm-thick (**a**) steel or (**b**) Kapton foil substrates at three deposition temperatures $T_d = 150°C$, $200°C$, and $250°C$

tensile strain in the film is needed to compensate for the CTE mismatch between the substrate and the film.

2.3.3 Radius of Curvature R of the Workpiece

When $Y_f\, d_f << Y_s\, d_s$, the substrate dominates and the film complies with it, as a TFT does on a plate glass substrate. The stress in the substrate is negligible, and the film/substrate couple curves only slightly, even when the film is highly stressed. The strain is biaxial in the plane of the film, and the structure forms a spherical cap with the radius of curvature given by:

$$R = \frac{d_s}{6\frac{Y_f^* d_f}{Y_s^* d_s}\left(e_f - e_s\right)} \cdot \frac{\left(1 - \frac{Y_f^* d_f^2}{Y_s^* d_s^2}\right)^2 + 4\frac{Y_f^* d_f}{Y_s^* d_s}\left(1 + \frac{d_f}{d_s}\right)^2}{1 + \frac{d_f}{d_s}} \quad (2.14)$$

where $(e_f - e_s)$ is the mismatch strain between the film and the substrate. The mismatch strain has two dominant components. One is the thermal mismatch strain caused by the difference between the CTE of the substrate, α_s, and that of the film, α_f. The other is the built-in strain ε_{bi} grown into the film during its deposition. Therefore,

$$e_f - e_s = \alpha_f \cdot (T_r - T_d) + \varepsilon_{bi} - \alpha_s \cdot (T_r - T_d) = \left(\alpha_f - \alpha_s\right)\cdot(T_r - T_d) + \varepsilon_{bi} \quad (2.15)$$

where $(T_r - T_d)$ is the difference between the room and the deposition temperatures. $R > 0$ when the film is on the convex side and $R < 0$ when the film is on the concave side of the film-on-foil structure. When $e_f - e_s = 0$, $R \to \infty$, and the structure becomes flat.

Since $Y_f\, d_f << Y_s\, d_s$, the second fraction in Eq. (2.14) is typically neglected, leading to the Stoney formula:

$$R = \frac{d_s}{6\frac{Y_f^* d_f}{Y_s^* d_s}\left(e_f - e_s\right)} \quad (2.16)$$

In such cases, R is very large.

A stiff film and a compliant substrate, for example an a-Si:H layer on an organic polymer foil, may have similar products of elastic modulus and thickness, $Y_f\, d_f \approx Y_s \cdot d_s$. The structure rolls into a cylinder instead of forming a spherical cap. An example is shown in Fig. 2.8, for a 500-nm-thick layer of SiN$_x$ deposited on two different plastic substrates by PECVD at 150°C.

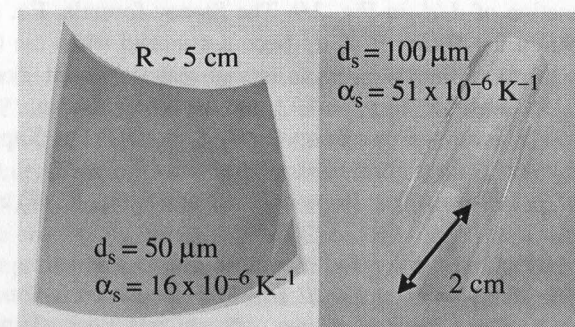In such a case, the Stoney formula is no longer valid. The radius of curvature R is now given by [9]:

Fig. 2.8 500-nm-thick PECVD SiN$_x$ film deposited on two different plastic substrates. The substrate thickness and the CTE are shown for each substrate. The film is deposited on the top and the structures roll into cylinders. The *left* picture shows the SiN$_x$ film in tension, and the *right* one in compression [9]

$$R = \frac{d_s}{6\frac{Y'_f d_f}{Y'_s d_s}(e_f - e_s)} \cdot \left\{ \frac{\left[\left(1 - \frac{Y'_f d_f^2}{Y'_s d_s^2}\right)^2 + 4\frac{Y'_f d_f}{Y'_s d_s}\left(1 + \frac{d_f}{d_s}\right)^2\right]\left[(1-\nu_s^2) + \left(\frac{Y'_f d_f}{Y'_s d_s}\right)^2(1-\nu_f^2)\right]}{\left(1 + \frac{d_f}{d_s}\right)\left(1 + \frac{Y'_f d_f}{Y'_s d_s}\right)\left[(1-\nu_s^2)(1+\nu_f) + \frac{Y'_f d_f}{Y'_s d_s}(1-\nu_f^2)(1+\nu_s)\right]} + \right.$$

$$\left. + \frac{3\left(\frac{Y'_f d_f}{Y'_s d_s}\right)^2\left(1 + \frac{d_f}{d_s}\right)^2\left[(1-\nu_s^2) + (1-\nu_f^2)\right] + 2\frac{Y'_f d_f}{Y'_s d_s}(1-\nu_s\nu_f)\left(1 + \frac{Y'_f d_f}{Y'_s d_s}\right)\left(1 + \frac{Y'_f d_f^3}{Y'_s d_s^3}\right)}{\left(1 + \frac{d_f}{d_s}\right)\left(1 + \frac{Y'_f d_f}{Y'_s d_s}\right)\left[(1-\nu_s^2)(1+\nu_f) + \frac{Y'_f d_f}{Y'_s d_s}(1-\nu_f^2)(1+\nu_s)\right]} \right\} \tag{2.17}$$

Here, $Y'_f = \frac{Y_f}{1-\nu_f^2}$ and $Y'_s = \frac{Y_s}{1-\nu_s^2}$ are the plane strain moduli of the film and the substrate, respectively. (During the derivation of Eq. (2.17), the $1/(1-\nu^2)$ factor accompanies each corresponding Young's modulus. Therefore, the introduction of the plane strain modulus $Y' = \frac{Y}{1-\nu^2}$ simplifies the expressions.)

If the Poisson ratios ν of the film and the substrate are identical, Eq. (2.17) simplifies to the form [7]:

$$R = \frac{d_s}{6\frac{Y_f d_f}{Y_s d_s}(e_f - e_s)(1+\nu)} \cdot \frac{\left(1 - \frac{Y_f d_f^2}{Y_s d_s^2}\right)^2 + 4\frac{Y_f d_f}{Y_s d_s}\left(1 + \frac{d_f}{d_s}\right)^2}{\left(1 + \frac{d_f}{d_s}\right)} \tag{2.18}$$

The mismatch strain $(e_f - e_s)$ is again given by Eq. (2.15). The first fraction in Eq. (2.18) is the Stoney formula divided by $(1+\nu)$, a factor arising from the generalized plane strain condition (cylindrical shape). The $(1+\nu)$ factor in the denominator of Eq. (2.18) reflects the observation that a compliant substrate rolls into a cylinder, rather than the spherical cap assumed in the Stoney formula. The second fraction is identical to that of Eq. (2.14) and constitutes the deviation from the Stoney formula for compliant substrates. When the mechanical properties of the film and the substrate and the radius of curvature R are known, one can extract the built-in strain ε_{bi} of the film [8].

The normalized radius of curvature, calculated from Eqs. (2.16) and (2.18), is plotted as a function of d_f/d_s in Fig. 2.9. The Stoney formula, Eq. (2.16), which is an approximation for $Y_f d_f \ll Y_s d_s$, becomes invalid when the film thickness approaches the substrate thickness, regardless of materials used. For typical TFT materials on a steel substrate, $Y_f/Y_s = 0.92$, and the Stoney formula with the $(1+\nu)$ factor included is a good approximation for $d_f/d_s \leq 0.01$. For Kapton substrate, $Y_f/Y_s = 35$, and the Stoney formula is useful only for $d_f/d_s \leq 0.001$. In the specific case of a 100-μm-thick Kapton E substrate, Eq. (2.18) must be used for $d_f > 100$ nm.

Figure 2.10 shows the film-on-foil curvature $1/R$ as a function of the built-in strain in the film calculated using Eq. (2.18). The calculation is done for a 1-μm-thick PECVD SiN$_x$ film deposited on two different substrates, stainless steel and Kapton E, at three deposition temperatures $T_d = 150°C$, $200°C$, and $250°C$. The following parameters were used in the calculations: $d_f = 1$ μm, $d_s = 100$ μm, $Y_f = 183$ GPa, $Y_s = 200$ GPa (steel) or 5.2 GPa (Kapton E), $\nu = 0.3$, $\alpha_f = 2.7 \times 10^{-6}$ K^{-1}, $\alpha_s = 18 \times 10^{-6}$ K^{-1} (steel) or 16×10^{-6} K^{-1} (Kapton E), and $T_r = 20°C$.

Fig. 2.9 Normalized radius of curvature as a function of film/substrate thickness ratio. *Full lines* are the solution for a cylindrical roll, Eq. (2.18), with $\nu = 0.3$. *Dashed* lines are the Stoney formula, Eq. (2.16), for a spherical cap formed by a thick, stiff wafer
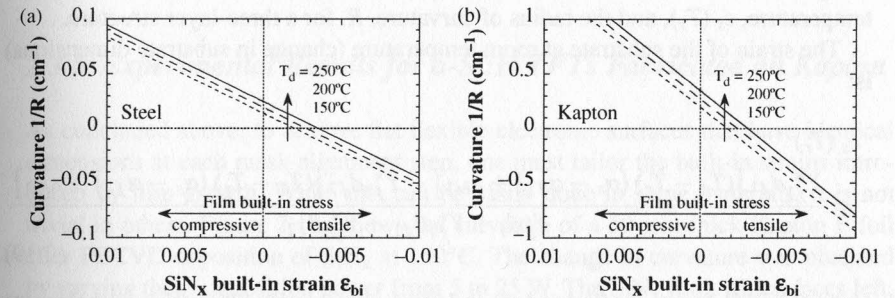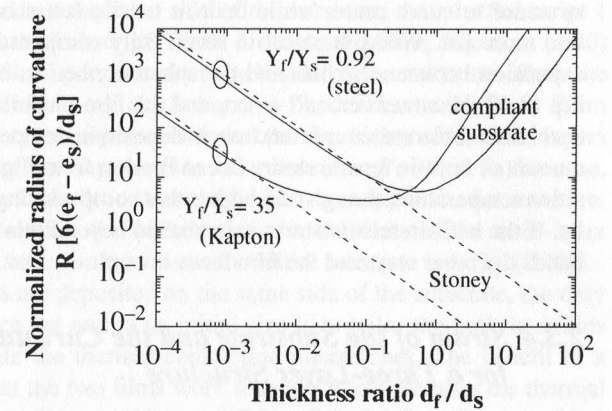
Fig. 2.10 Curvature $1/R$ of the film-on-foil structure at room temperature as a function of the built-in strain imposed by the film grown at an elevated temperature, calculated using Eq. (2.18). A 1-μm-thick PECVD SiN$_x$ film is deposited on two different substrates of a 100-μm-thick (a) steel or (b) Kapton E foil. The calculations are done for three different deposition temperatures T_d of 150, 200, and 250°C. The remaining parameters are listed in the text

A 100-μm-thick Kapton foil curves substantially more after the growth of a 1-μm-thick PECVD SiN$_x$ film than a 100-μm-thick stainless steel foil coated with an identical film. If the SiN$_x$ film is grown without built-in stress ($\sigma_{bi} = 0$ and $\varepsilon_{bi} = 0$), the structure curves with the film on the outside. The room-temperature curvature $1/R$ of the SiN$_x$-on-Kapton structure is 0.19 cm^{-1} ($R = 5.3$ cm) with a film grown at 150°C, 0.26 cm^{-1} ($R = 3.8$ cm) at 200°C, and 0.34 cm^{-1} ($R = 2.9$ cm) at 250°C. The room-temperature curvature $1/R$ of the SiN$_x$-on-steel structure is 0.013 cm^{-1} ($R \sim 77$ cm) with a film grown at 150°C, 0.019 cm^{-1} ($R \sim 53$ cm) at 200°C, and 0.025 cm^{-1} ($R \sim 40$ cm) at 250°C.

Both Kapton and steel have larger thermal expansion coefficients than the SiN$_x$ film. Upon cooling from the growth temperature, the substrate shrinks more than the SiN$_x$ film. The SiN$_x$ is forced to occupy the longer, outside perimeter of the cylindrical roll. Built-in compressive stress in the film forces the film-on-foil

structure to curve more, while built-in tensile stress in the film makes the structure more flat. When the built-in strain fully compensates the differential thermal expansion between the film and the substrate, i.e. $e_f - e_s = 0$, the denominator in Eq. (2.18) becomes zero. $R \to \infty$, and the film-on-foil structure becomes flat. For each film/substrate couple and each deposition temperature, there is an optimal amount of built-in tensile strain, as can be seen from Fig. 2.10. The higher the deposition temperature, though, the higher this compensating built-in tensile strain must be. If the built-in tensile strain is increased beyond this optimal point, the structure bends the other way, and the film faces inward.

2.3.4 Strain of the Substrate and the Curvature of the Workpiece for a Three-Layer Structure

The preceding theory can be extended easily to any number of layers. The layer design will benefit from a brief discussion of the strain of the substrate at room temperature, $\varepsilon_s (T_r)$, and the radius of curvature, R, for a three-layer structure.

The strain of the substrate at room temperature (change in substrate dimensions) is:

$$\varepsilon_s (T_r)$$
$$= \frac{Y_{f1}^* d_{f1} \left[(T_d - T_r)(\alpha_s - \alpha_{f1}) + \varepsilon_{bi1} \right] + Y_{f2}^* d_{f2} \left[(T_d - T_r)(\alpha_s - \alpha_{f2}) + \varepsilon_{bi2} \right]}{Y_s^* d_s + Y_{f1}^* d_{f1} + Y_{f2}^* d_{f2}}$$

$$(2.19)$$

Here, $f1$ and $f2$ denote the first and second films, respectively. The other symbols were introduced earlier. Equation (2.19) is valid whether each side of the substrate is coated with one film or both films are deposited on the same side. Similarly to a two-layer structure, the higher the deposition temperature and the larger the CTE mismatch between the substrate and either of the films, the larger must be the compensating built-in tensile strain. $\varepsilon_s (T_r) \neq 0$ unless the built-in strains induced by the growing films are tailored appropriately.

If the Poisson ratio ν is the same for all layers, the radius of curvature R of the relaxed three-layer structure (see Fig. 2.11) at room temperature is given by:

$$R = \frac{d_1}{6(1+\nu)} \cdot$$
$$\left\{ \frac{\left(1 - \frac{Y_2 d_2^2}{Y_1 d_1^2} - \frac{Y_3 d_3^2}{Y_1 d_1^2}\right)^2 + 4\frac{Y_2 d_2}{Y_1 d_1}\left(1 + \frac{d_2}{d_1}\right)^2 + 4\frac{Y_3 d_3}{Y_1 d_1}\left[\left(1 + \frac{d_3}{d_1}\right)^2 + 3\frac{d_2}{d_1}\left(1 + \frac{d_2}{d_1} + \frac{d_3}{d_1}\right) + \frac{Y_2 d_2}{Y_1 d_1}\left(\frac{d_2^2}{d_1^2} + \frac{d_2 d_3}{d_1^2} + \frac{d_3^2}{d_1^2}\right)\right]}{\left(1 + \frac{d_2}{d_1}\right)\left[\frac{Y_2 d_2}{Y_1 d_1}(e_2 - e_1) + \frac{Y_3 d_3}{Y_1 d_1}(e_3 - e_1)\right] + \frac{Y_3 d_3}{Y_1 d_1}\left(\frac{d_2}{d_1} + \frac{d_3}{d_1}\right)\left[(e_3 - e_1) + \frac{Y_2 d_2}{Y_1 d_1}(e_3 - e_2)\right]} \right\}$$

$$(2.20)$$

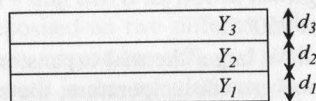| Y_3 | $\updownarrow d_3$ |
| Y_2 | $\updownarrow d_2$ |
| Y_1 | $\updownarrow d_1$ |

Fig. 2.11 Three-layer structure

If both layers are deposited on the same side of the substrate, then the Subscript 1 denotes the substrate and the Subscripts 2 and 3 denote the films. Equation (2.20) can also be used if one film is deposited on each side of the substrate. Then the Subscript 2 denotes the substrate and the Subscripts 1 and 3 denote the films. From analyzing Eq. (2.20), one can easily conclude that the deposition of identical layers on both sides of the substrate always leads to a flat structure ($R \to \infty$). In this case, it is not necessary to tailor the built-in strain in the films to achieve the flat structure. However, it is essential to tailor the built-in strain in the films, if the three-layer structure should have the same dimensions as the initial substrate (see Eq. (2.19)).

If two dissimilar layers are deposited on the same side of the substrate, the only way to keep the workpiece flat and at its initial size is to tailor the built-in strains in the films to compensate the thermal contraction mismatches. The benefit of a three-layer structure is that the two films work together to compensate the thermal mismatch. It becomes possible to achieve $\varepsilon_s (T_r) = 0$ and $1/R = 0$, even if the deposition of each film separately leads to $\varepsilon_s (T_r) \neq 0$ and $1/R \neq 0$.

2.3.5 Experimental Results for a-Si:H TFTs Fabricated on Kapton

As concluded above, to achieve flat flexible electronic surfaces that have identical dimensions at each mask alignment step, one must tailor the built-in strains introduced by film growth. While this can be easily done in some materials, it is not trivial in others. Figure 2.12a shows the curvature of a 50-μm-thick Kapton E foil after PECVD deposition of SiN_x at 150°C. The change in curvature was obtained by varying the rf deposition power from 5 to 25 W. The SiN_x film, which faces left, is under tension for low deposition power and under compression for the highest deposition power. Figure 2.12b shows two other materials, Cr and a-Si:H, whose built-in strains are difficult to vary. Cr is typically under tension and a-Si:H under compression.
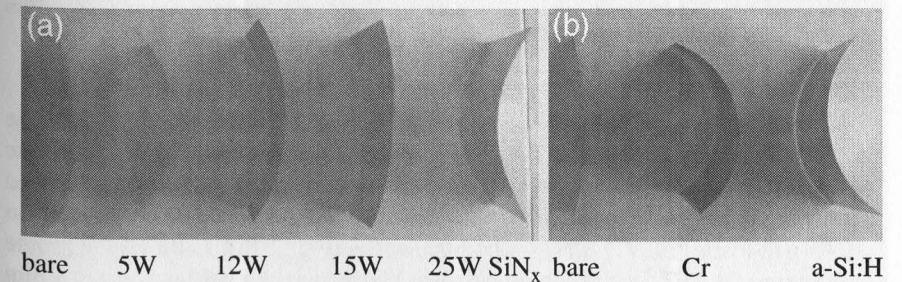

bare   5W   12W   15W   25W SiN_x   bare   Cr   a-Si:H

Fig. 2.12 Curvature induced by (**a**) SiN_x deposited over a range of rf power and (**b**) Cr and a-Si:H, all on 50-μm-thick Kapton E polyimide substrates. All films are facing *left*. The 300−500-nm-thick SiN_x and the 250-nm-thick a-Si:H films were deposited at 150°C, and the 80-nm-thick Cr was deposited by thermal evaporation without control of substrate temperature. The bare substrate is also shown for comparison [8]
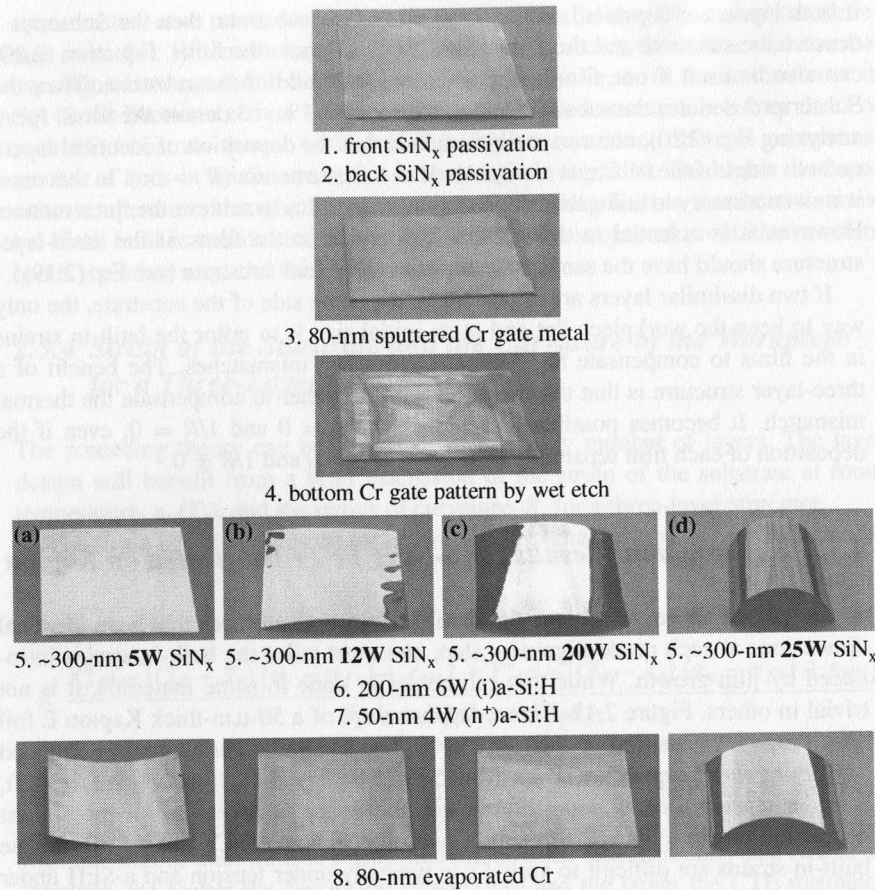
1. front SiN$_x$ passivation

2. back SiN$_x$ passivation

3. 80-nm sputtered Cr gate metal

4. bottom Cr gate pattern by wet etch

(a)   (b)   (c)   (d)

5. ~300-nm **5W** SiN$_x$ 5. ~300-nm **12W** SiN$_x$ 5. ~300-nm **20W** SiN$_x$ 5. ~300-nm **25W** SiN$_x$

6. 200-nm 6W (i)a-Si:H

7. 50-nm 4W (n$^+$)a-Si:H

8. 80-nm evaporated Cr

Fig. 2.13 Curvature variation in a-Si:H TFT fabrication on Kapton foil at five steps from substrate passivation to evaporation of the top Cr source/drain contact metal. For all four samples, the entire process is identical except for the deposition of the gate SiN$_x$, where the rf power was varied from 5 to 25 W. The square substrate is 7.5×7.5 cm^2 [8]

The ability to vary the built-in strain in SiN$_x$ over a wide range was put to use in TFT fabrication such that the gate and source/drain patterns aligned. Complete a-Si:H TFTs were fabricated at 150°C in a non-self-aligned, back-channel-etched geometry. We began by passivating a 50-μm-thick Kapton E substrate foil with an ~0.45-μm-thick PECVD SiN$_x$ on both sides (see Fig. 2.13). Following substrate passivation, the TFT fabrication process was carried out. An ~80-nm-thick Cr film was sputtered at room temperature and wet etched to create the first device pattern, the bottom gate electrode. All samples are flat after this first Cr evaporation. Next, a silicon stack composed of ~300-nm SiN$_x$ gate dielectric layer, ~200-nm (i)a-Si:H channel layer, and ~50-nm (n$^+$)a-Si:H source/drain layer was deposited by PECVD, followed by ~80-nm-thick thermally evaporated Cr for the source/drain

metal contacts. The details of fabrication are described elsewhere [8]. Note that only sample (a) is flat after the SiN$_x$/(i)a-Si:H/(n$^+$)a-Si:H stack deposition. If a mask were aligned to the gate pattern at this step, sample (a) would experience the smallest misalignment error. However, the situation changes after the source/drain Cr is evaporated, which makes samples (b) and (c) flat instead. This sequence shows that all four device layers work together to compensate the CTE mismatch.

We measured the misalignment between the first and second photolithography levels, i.e. the bottom gate and the top source/drain. Steps 5–8 of Fig. 2.13 fall between these two photolithographic steps. In all four samples of Fig. 2.13, we kept these layers the same, except for intentionally varying the built-in stress in the gate
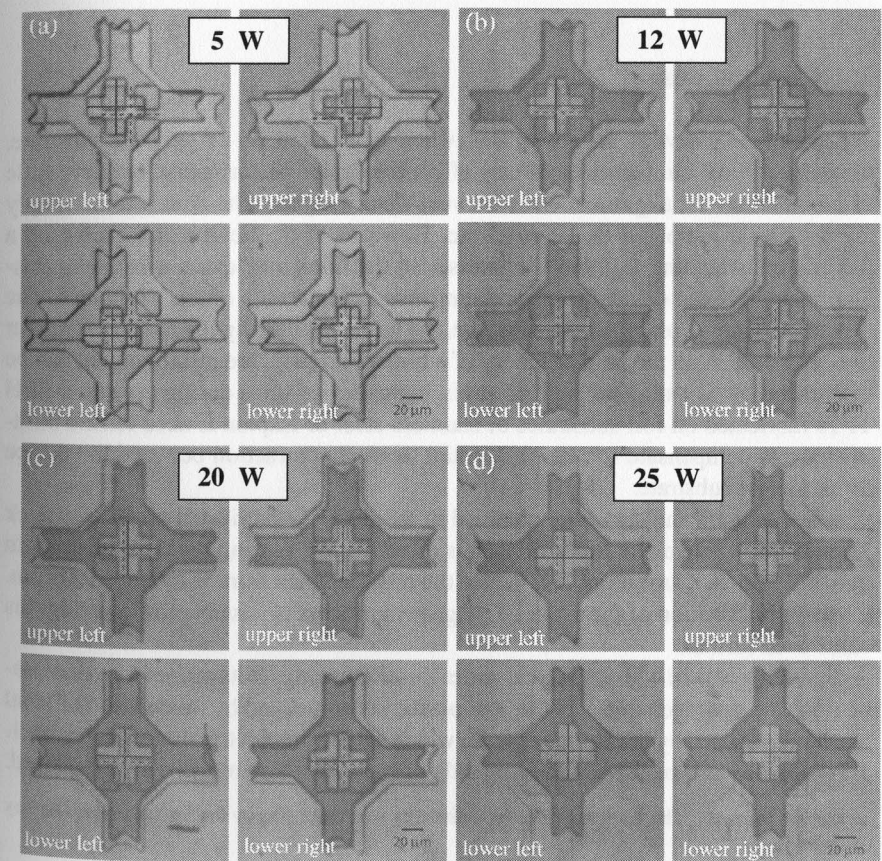

Fig. 2.14 Overlay misalignment between the first, gate, and the second, source/drain, photolithography levels in the back-channel-etched a-Si:H TFT process with (**a**) 5 W, (**b**) 12 W, (**c**) 20 W, and (**d**) 25 W gate SiN$_x$. The frames lie 52 mm apart near the corners of the substrate. The *dashed* crosses mark the centers of the alignment marks at the gate level and the *solid black* crosses, at the source/drain level [8]

SiN_x by tuning the rf deposition power from low to high, 5, 12, 20, and 25 W (22, 53, 89, and 111 mW/cm^2).

Figure 2.14 shows the corresponding alignment marks for the gate and the source/drain for all four samples. Both the gate and the source/drain patterns were aligned at the center of the substrate, and the misalignment was measured on alignment marks in four corners of a 52-mm × 52-mm square. These marks are shown in Fig. 2.14. The centers of the alignment marks are indicated by dashed crosses for the gate level and solid crosses for the source/drain. On average, sample (a) shrunk substantially, by ∼480 ppm, sample (b) shrunk slightly, by ∼96 ppm, sample (c) expanded slightly, by ∼115 ppm, and sample (d) expanded substantially, by ∼385 ppm. As expected, the dimensions for the flat samples (b) and (c) changed the least. As fabricated, TFTs of all samples had similar electrical performance.

2.4 Conclusions

When inorganic devices are grown at elevated temperature on a rigid plate substrate, the device films' built-in stresses may affect the device performance, but have little or no effect on the alignment error between device layers. The device films simply are too weak compared to the substrate. However, if the devices are grown on a flexible free-standing foil, built-in stresses in the films may cause substantial misalignment between device layers and unmanageable curving of the workpiece. The thinner and more compliant the substrate, the larger the misalignment and the tighter the curvature. With the help of theory of a bimetallic strip, the misalignment can be minimized by adjusting the built-in strain in the device films during growth. a-Si:H TFTs fabricated on foil substrates of stainless steel or Kapton E need tensile built-in strain to compensate for the differential thermal contraction between the device films and the substrate.

Misalignment and curvature obtained in a-Si:H TFTs fabricated on 50-μm-thick Kapton E foil prove that this approach is effective. By varying the built-in strain in only the gate SiN_x layer, one can reduce the misalignment from ∼400 to ∼100 ppm. Further optimization of the a-Si:H TFT growth process is possible for lowering this value even further.

Future work will address second-order misalignment effects caused by viscoelastic flow and nonreversible shrinkage of plastic substrate, and by modulation of local mechanics caused by device patterns. To which extend the electrical and the mechanical properties may be varied independently of each other also remains to be explored.

References

1. Crawford GP (ed) (2005) Flexible Flat Panel Displays. Wiley, Chichester
2. Hutchinson JW, Suo Z (1991) Mixed-mode cracking in layered materials. Adv Appl Mech 29:63–191

3. Jansen F, Machonkin MA (1988) Thermomechanical properties of glow discharge deposited silicon and silicon oxide films. J Vac Sci Technol A6:1696–1698
4. Maeda M, Ikeda K (1998) Stress evaluation of radio-frequency-biased plasma-enhanced chemical vapor deposited silicon nitride films. J Appl Phys 83:3865–3870
5. Witvrouw A, Spaepen F (1993) Viscosity and elastic constants of amorphous Si and Ge. J Appl Phys 74:7154–7161
6. Freund LB, Suresh S (2003) Thin film materials. Cambridge University Press, New York
7. Suo Z, Ma EY, Gleskova H, Wagner S (1999) Mechanics of rollable and foldable film-on-foil electronics. Appl Phys Lett 74:1177–1179
8. Cheng I-C, Kattamis A, Long K, Sturm JC, Wagner S (2005) Stress control for overlay registration in a-Si:H TFTs on flexible organic polymer foil substrates. J SID 13:563–568
9. Gleskova H, Cheng I-C, Wagner S, Sturm JC, Suo Z (2006) Mechanics of thin-film transistors and solar cells on flexible substrates. Solar Energy 80:687–693